Inorganic Chemistry

Article

pubs.acs.org/IC

Turning on Lanthanide Luminescence via Nanoencapsulation

Boris Makhinson,[†] Alexandra K. Duncan,[†] Ashley R. Elam,[†] Ana de Bettencourt-Dias,[‡] Colin D. Medley,[§] Joshua E. Smith,*[,†] and Eric J. Werner*[,∥]

[†]Department of Chemistry and Physics, Armstrong Atlantic State University, 11935 Abercorn Street, Savannah, Georgia 31419, United States

[‡]Department of Chemistry, University of Nevada, Reno, Nevada 89557, United States

[§]Genentech Inc., Small Molecule Pharmaceutical Sciences, 1 DNA Way, South San Francisco, California 94080, United States

[∥]Department of Chemistry, Biochemistry and Physics, The University of Tampa, 401 W. Kennedy Boulevard, Tampa, Florida 33606, United States

Supporting Information

ABSTRACT: Encapsulation of macrocyclic europium(III) chelates by discrete, monodisperse SiO_2 nanoparticles (NPs) has been carried out, and the resulting significant enhancement of metal-derived luminescence has been studied to rationalize this dramatic effect. The tetraiminodiphenolate motif chosen for this study is easily synthesized and incorporated into the NP matrix under ambient conditions. The free complex exhibits primarily weak ligand-derived emission at room temperature, typical for these compounds, and displays intense metal-centered luminescence from the europium only when cooled to 77 K. Upon encapsulation by the NPs, however, europium-derived luminescence is visibly "turned on" at room temperature, yielding strong emission peaks characteristic of europium(III) with a corresponding enhancement factor of 6×10^6. The similar ligand singlet and triplet excited-state energies determined for the free complex (20820 and 17670 cm^{-1}, respectively) versus the encapsulated complex (20620 and 17730 cm^{-1}) indicate that encapsulation does not affect the energy levels of the ligand appreciably. Instead, a detailed analysis of the metal-centered emission and ligand singlet and triplet emission bands for the free and encapsulated complexes reveals that the enhanced metal emission is due to the rigid environment afforded by the silica NP matrix affecting vibrationally mediated energy transfer. Further, the metal-centered emission lifetimes in methanol versus deuterated methanol indicate a decrease in the number of coordinated solvent molecules upon encapsulation, changing from an average of 3.3 to 2.1 bound methanol molecules and reducing the known quenching effect on europium-centered luminescence due to nearby OH vibrations.

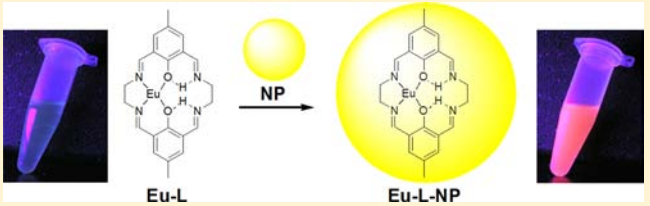

INTRODUCTION

The incorporation of lanthanide (Ln) metal ions into functional nanomaterials has received increasing attention, with emerging applications ranging from the development of advanced optical materials[1−3] to biomedical imaging.[4,5] Luminescence derived from Ln ions presents distinct advantages over emission from organic chromophores because of the characteristic and narrow emission peaks, large Stokes shifts of the sensitized emission, and relatively long lifetimes exhibited by the lanthanides.[6] Combining these favorable characteristics of Ln luminescence with the diverse applicability of functionalizable silica-based nanoparticles (NPs) therefore presents an attractive approach toward the development of next-generation emissive materials. Further, such nanoencapsulation may lead to an improvement of the basic photophysical properties of the Ln-based species, as has been noted previously.[7,8] Enhanced luminescence is particularly desirable if intense Ln-centered emission can be generated from combining relatively simple precursors via straightforward means, thus providing a convenient route toward optimized emission from lanthanide chelates to fully exploit their utility.

While Ln compounds have been studied in a variety of doping methodologies within nanomaterial systems, many of these investigations have focused on the incorporation of simple lanthanide salts which are typically doped into NP frameworks.[9−12] Encapsulation of well-characterized Ln complexes employing multidentate chelating chromophores instead of simple salts can be advantageous in that these chromophores promote the so-called "antenna effect", where light is harvested by the organic ligand and transferred from a triplet excited state to the metal ion before being emitted as visible light.[6] This effect circumvents the low molar absorptivities of the ions themselves that result in weak luminescence intensities of simple inorganic lanthanide salts. Moreover, the introduction of the Ln in a chelated form into an SiO_2 NP matrix versus Ln-ion doping or via particle surface modification[13,14] should discourage the release or leaching of the metal, an important consideration particularly for any biological application. The straightforward, noncovalent encapsulation of lanthanide

Received: October 16, 2012
Published: May 21, 2013

   dx.doi.org/10.1021/ic3022722 | Inorg. Chem. 2013, 52, 6311−6318

chelate complexes within discrete, well-characterized SiO_2 NPs has been reported.[7,15−18] These studies avoid the more cumbersome covalent particle modifications requiring multistep syntheses, a desirable characteristic with regard to practical application. Despite reports of such efforts, well-defined Ln/SiO_2 NP systems are seldom prepared using chelating ligands of high denticity. Furthermore, reports of hybrid Ln−nanomaterial systems often focus on the generation of solid-state glasses or films versus discrete, monodisperse particles and exhibit metal-derived luminescence that is either unaffected or enhanced to only a modest extent relative to the free Ln compound.[19,20]

The implementation of chelating macrocyclic ligands, not yet utilized in such an approach with monodisperse NPs, would afford highly stable chelates suitable for application in nanomaterials. We have therefore turned our attention to macrocyclic Ln complexes, exploring in particular the tetraiminodiphenolate (TIDP; Scheme 1) motif. Such TIDP ligands have been used extensively in transition-metal complexation[21,22] but have received far less attention as Ln chelators. Considering the relatively simple synthetic procedures using inexpensive starting materials and expected high chelate stability, Ln-TIDP complexes are attractive as practical candidates for NP encapsulation and further application. One drawback, however, arises in considering the known luminescence properties of such complexes. While the photophysical characteristics of Ln-TIDP complexes still remain largely overlooked, Nag and co-workers have reported several emission spectra of one TIDP ligand coordinated to Eu^{3+} and Sm^{3+}.[23] For solutions of such complexes, ligand emission is predominantly observed at room temperature, and efficient energy transfer and subsequent metal-centered emission can only be achieved at low temperature (reported spectra collected at 77 K). Given the straightforward synthesis of the TIDP metal complexes combined with the ease at which structural variations can be pursued to tune for specific applications, the improvement of the photophysical aspects of this ligand system presents itself as a worthwhile goal. This study aims to utilize the basic TIDP ligand framework to obtain a europium(III) complex and provide a detailed account and rationalization of the dramatic effect of SiO_2 NP encapsulation on the luminescence properties of the complex within a new nanocomposite material.

Scheme 1. Synthesis of Eu-L[a]

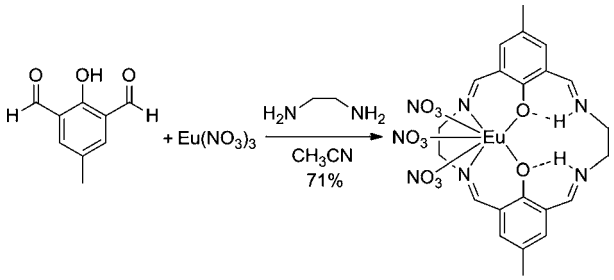

[a]The known bidentate binding mode of the coordinated nitrate ions is not depicted in the structure here for clarity.

EXPERIMENTAL SECTION

Chemicals and Instrumentation. All chemicals were received from Sigma-Aldrich and used without further purification unless otherwise noted. Ammonium hydroxide and tetraethylorthosilicate (TEOS) were purchased from Fisher, Inc. 4-Methyl-2,5-diformylphenol was synthesized as previously reported[24,25] Elemental (CHN) analyses were performed by Atlantic Microlab Inc. (Norcross, GA), and Fourier transform infrared (FT-IR) spectra were obtained using a Perkin-Elmer Spec. 100 spectrometer fitted with the ATR sampling accessory. The scanning electron microscopy (SEM) images were obtained using a Zeiss SEM Ultra60 scanning electron microscope.

Synthesis of Eu-L. A solution of ethylenediamine (80.4 μL, 1.2 mmol) and europium(III) nitrate hydrate (0.238 g, 0.55 mmol) in acetonitrile (50 mL) was added to a solution of 4-methyl-2,5-diformylphenol (0.200 g, 1.2 mmol) in acetonitrile (50 mL) at room temperature under stirring. A yellow precipitate was seen in the flask within minutes, and stirring was continued overnight. The solid product was filtered, washed with acetonitrile, and dried in vacuo (0.293 g, 71.0%). Anal. Calcd for **Eu-L**·H_2O·CH_3CN (found): C, 37.27 (37.02); H, 3.78 (3.94); N, 14.49 (14.82). FT-IR (cm^{-1}): 3375 w br, 1654 s, 1632 s, 1539 m, 1488 m, 1463 m, 1444 m, 1419 m, 1367 m, 1328 m, 1299 s, 1279 s, 1231 s, 1121 m, 1090 w, 1042 m, 1034 m, 993 m, 855 m, 816 m, 780 w, 737 w, 679 w. UV−vis in 4:1 EtOH/MeOH [λ_{max} (nm), ε (M^{-1} cm^{-1})]: 250, 41680; 399, 14724.

Luminescent NP Synthesis. **Eu-L** encapsulated NPs were synthesized via the Stöber method. In a 15 mL glass vial, 4.19 mL of absolute ethanol was added followed by 239 μL of NH_4OH with continuous stirring, 2 mg of **Eu-L**, and 210 μL of TEOS. The mixture was allowed to stir vigorously in a covered environment for 48 h. After the stirring period, the sample was washed three times with ethanol. First, the sample was centrifuged at 14000 rpm for 20 min, the supernatant was decanted, and 1 mL aliquots of ethanol were added. After addition of the fresh ethanol, the NPs were suspended by sonication. This procedure was repeated for all washing steps. After the final centrifugation, the samples were suspended in 1 mL of ethanol and the concentration was determined. For SEM imaging, 1 μL of the NP solution was diluted to 1000 μL with ethanol for analysis.

Photophysical Measurements. Solvents were dried by standard methods, and solutions were prepared in a Nexus glovebox under a controlled nitrogen atmosphere (O_2 < 0.2 ppm; H_2O < 1 ppm). They were allowed to equilibrate for at least 2−3 h before measurements. Unless otherwise indicated, all data were collected at a constant temperature of 25.0 ± 0.1 °C. All measurements were performed in triplicate over a period of several days, and the lifetime measurements were repeated and found to be consistent after 6 months.

Excitation and emission spectra were measured on a Perkin-Elmer LS-55 fluorescence spectrometer equipped with a xenon flash lamp. Measurements were done in the phosphorescence mode with a delay of 0 ms after lamp pulse, a cycle time of 16 ms, a gate time of 0.05 ms, and a flash count of 1. Slit widths were 5 and/or 10 nm, and a scan rate of 250 nm s^{-1} was used. The triplet state measurements were performed at 77 K, as described by Crosby et al.[26] The triplet state energy is indicated as the 0−0 transition after deconvolution of the phosphorescence spectrum into its Franck−Condon progression. All emission and excitation spectra were corrected for instrumental function. The excitation wavelength was 315 nm. A Shimadzu RF-5301 spectrofluorometer was used to collect the emission spectra shown in Figures 1 and 4, using the parameters and solvents specified.

Lifetimes were measured on a Horiba Jobin-Yvon Fluoro-3 fluorescence spectrometer equipped with a xenon flash lamp. An initial delay of 0.06 ms, a sample window of 2 ms, a maximum delay of 3 s, a delay increment of 0.01 ms, a time per flash of 41 ms, and a flash count of 100 were applied, with an integration time of 100 ms. The excitation wavelength was 315 nm.

Leaching Study. The Eu-L@SiO_2 NPs were prepared as described above and investigated for leaching of **Eu-L** from the particles. The study was performed by diluting 100 μL aliquots of a sample of particles to 1 mL with ethanol into 10 separate microcentrifuge tubes. Over the course of 6 weeks, samples from the set were centrifuged at

dx.doi.org/10.1021/ic3022722 | Inorg. Chem. 2013, 52, 6311−6318

14000 rpm for 20 min each. After centrifugation, the supernatant was decanted and analyzed using UV−vis spectrophotometry. The absorption spectra were obtained using a Hewlett-Packard 8453 spectrophotometer at wavelengths monitored from 300 to 750 nm. The absorbance obtained for each sample at 400 nm was exported to Microsoft Excel for analysis.

Inductively Coupled Plasma Mass Spectrometry (ICP-MS) Analysis. ICP-MS samples were prepared by aliquoting 100 μL of each NP suspension into a 15 mL conical tube. A total of 100 μL of reverse Aqua Regia was then added to the tube. Reverse Aqua Regia was prepared by the volumetric addition of 5 mL of HCl (Fluka TraceSelectUltra) to 15 mL of HNO_3 (Fluka TraceSelectUltra). Leaching samples were prepared by centrifuging the NPs for 20 min at 14000 rpm and aliquoting 1.00 mL of each solution into a 15 mL conical tube. After incubation for 18 h at room temperature, 100 μL of a scandium internal standard (BDH Aristar) was added to the samples, followed by 5 mL of Milli-Q water. Elemental standards for silicon (EMD CertiPur) and europium (BDH Aristar Plus) were prepared by adding 100 μL of each standard to a 15 mL conical tube followed by 100 μL of the scandium internal standard. A total of 5 mL of Milli-Q water was then added to each elemental standard tube. For all ICP-MS samples, an Agilent 7500 inductively coupled plasma mass spectrometer with an Agilent ASX-500 Series autosampler was used for analysis. The instrument was run in no-gas mode, monitoring m/z 28 for silicon, m/z 45 for scandium, and m/z 153 for europium and taking six repeating scans at each m/z. The injector was rinsed for 90 s between samples to eliminate carryover. Prior to analysis of the samples, the instrument was tuned using a 1 ppb tuning solution (Agilent Technologies 5185-5959). The raw data were then exported to Microsoft Excel for analysis. The elemental composition for each sample was determined using the elemental standards as a reference after normalization by the internal standard.

For quantification of Eu/NP, 1 mg samples of the Eu-L@SiO_2 NPs were digested and subsequently analyzed as described above for the leaching study. The Eu/NP content was calculated by dividing the amount of europium as determined by ICP-MS by the number of NPs digested in the sample.

RESULTS AND DISCUSSION

Synthesis and Characterization of Eu-L. With the goals of gaining a deeper understanding of the photophysical properties of Ln-TIDP complexes and ultimately utilizing the motif in luminescence applications under practical conditions, we have prepared the complex **Eu-L** (Scheme 1). The synthetic approach chosen to obtain **Eu-L** involves a convenient metal-templated reaction,[27] combining 1 equiv each of the dialdehyde and diamine linker with 0.5 equiv of the metal nitrate salt in one step to form the new macrocyclic complex in reasonable yield. When acetonitrile is used as the reaction solvent, the pure complex begins to precipitate from the solution minutes after mixing the reagents, with the product filtered as a yellow solid after allowing for complete precipitation. On the basis of the reported X-ray crystal structures of other Ln-TIDP complexes[28,29] and the large size of the macrocyclic cavity of the current ethyl-linked ligand relative to the europium(III) ion, it is expected that the europium(III) is coordinated by only four of the possible six donor atoms offered by the ligand, as shown in Scheme 1. To fully satisfy the inner coordination sphere of the metal, the nitrates introduced with the lanthanide salt during synthesis also bind the metal in a bidentate fashion, as discussed further below. The total coordination number of 10 for **Eu-L** resulting from the expected four ligand donors and three bidentate nitrates is reasonable for europium(III) and consistent with a closely related samarium(III) complex utilizing a similar TIDP motif.[28] Successful macrocyclic complex formation was confirmed by IR spectroscopy, noting the appearance of intense bands at 1654 and 1632 cm^{-1} corresponding to the coordinated and uncoordinated imine groups generated upon condensation (Figure S1, Supporting Information). UV−vis absorption (Figure S2, Supporting Information) and CHN elemental analysis were also used to confirm isolation of the desired product.

In addition to providing evidence of complex formation, analysis of the IR spectrum of **Eu-L** (Figure S1, Supporting Information) can also reveal the number and binding modes of nitrate ions present within the complex in the solid state. First, the absence of the characteristic strong peak in the range of 1380−1390 cm^{-1} indicates that there are no outer-sphere, ionic nitrates[27,30] confirming that all three nitrate groups are bound to the europium(III) center of **Eu-L**. Additionally, the relative location of the IR bands corresponding to the metal-bound nitrates can be used to distinguish between mono- and bidentate coordination modes of the ion. For example, the separation between the two highest frequency bands, ν(N═O) (ν_1) and $\nu_{asym}(NO_2)$ (ν_5), can be used to assess the degree of covalency for coordinated nitrate ions and is known to increase as nitrate coordination switches from mono- to bidentate.[31] In the case of **Eu-L**, the ν_1 and ν_5 bands appear at 1488 and 1299 cm^{-1}, respectively, with a $\Delta\nu$ value of 189 cm^{-1}, which indicates bidentate nitrate coordination. The presence of an IR band at 1034 cm^{-1}, corresponding to the $\nu_{sym}(NO_2)$ vibration of a covalent nitrate, further confirms bidentate coordination[32] and is consistent with an overall 10-coordinate structure.

Photophysical Studies of Eu-L. Emission spectra of a solution of **Eu-L** obtained at room temperature and 77 K are shown in Figure 1. An excitation wavelength of 400 nm was chosen for analysis and is consistent with the significant peak seen in the UV−vis absorption spectrum resulting from an internal ligand transition (Figure S2, Supporting Information). The overall emission intensity is significantly lower for the solution at room temperature, and while some metal-based emission is observed at 615 nm, characteristic of the europium(III) $^5D_0 \rightarrow {}^7F_2$ transition, ligand emission clearly dominates with a broad peak centered around 500 nm (see inset of Figure 1). Upon cooling to 77 K, metal emission is enhanced considerably to reveal the five peaks typically seen for europium-derived emission corresponding to transitions from

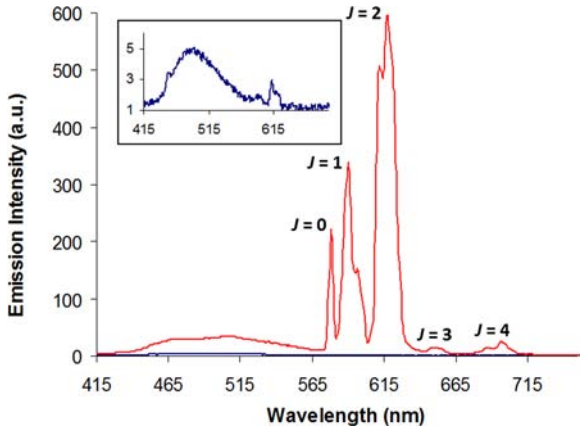

Figure 1. Emission spectra of **Eu-L** in 4:1 EtOH/MeOH collected at room temperature (blue) and at 77 K (red) (λ_{ex} = 400 nm). The europium(III) emission peaks are assigned as the expected $^5D_0 \rightarrow {}^7F_J$ transitions. Inset: same room temperature spectrum rescaled, revealing the dominant ligand emission peak.

dx.doi.org/10.1021/ic3022722 | Inorg. Chem. 2013, 52, 6311−6318

the $^5D_0$ level to the ^7F_J manifold (J = 0–4). The appearance of these pronounced metal-centered emission peaks at low temperature is attributed to more efficient energy transfer from the ligand to the metal because of decreased thermal repopulation of the ligand triplet state. To confirm this hypothesis, the triplet and singlet state energies of the ligand in the complex were determined (Figure 2) and are given in Table

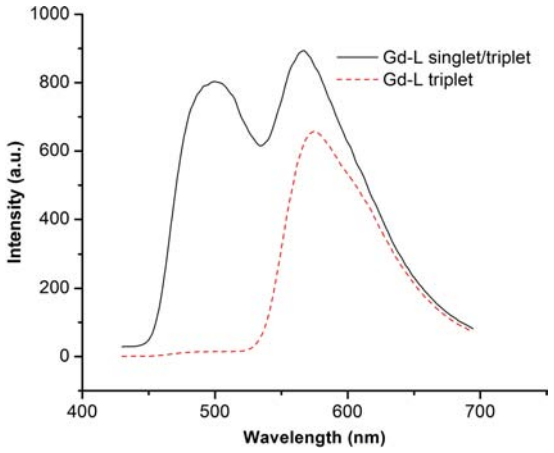

Figure 2. Fluorescence and phosphorescence spectra of **Gd-L** for determination of the triplet and singlet states. Spectra were collected for samples in MeOH at 77 K.

1. The singlet state is located at 20820 cm^{-1} and the triplet state at 17670 cm^{-1}. The triplet state is very close in energy to the emissive state of europium(III) (17300 cm^{-1}), which is therefore a good indicator of extensive vibrationally mediated back energy transfer. Because the back-transfer decreases with decreasing temperature, an improvement of metal-centered emission is expected and observed.[33,34] The emission lifetime monitored at 612 nm can be fit to a double exponential at room temperature (Figure 3), with the component of 347 μs corresponding to $^5D_0$ emission and the shorter lifetime of 35 μs being attributed to ligand-centered emission due to back transfer from the metal center. Given the presence of some ligand background emission at 612 nm, the two components of the emission lifetime were attributed to metal- and ligand-centered emission as opposed to emission of two europium(III) ions in two different sites. Such an interpretation is consistent with other studies[35−37] as well as the two significantly different lifetimes determined here along with no evidence of different europium(III) sites. As expected in the case of vibrationally assisted back-transfer, cooling the sample to 77 K yields a single-exponential decay with a lifetime of 1.063 ms, attributed solely to metal emission. A biexponential decay at room temperature was also detected upon monitoring

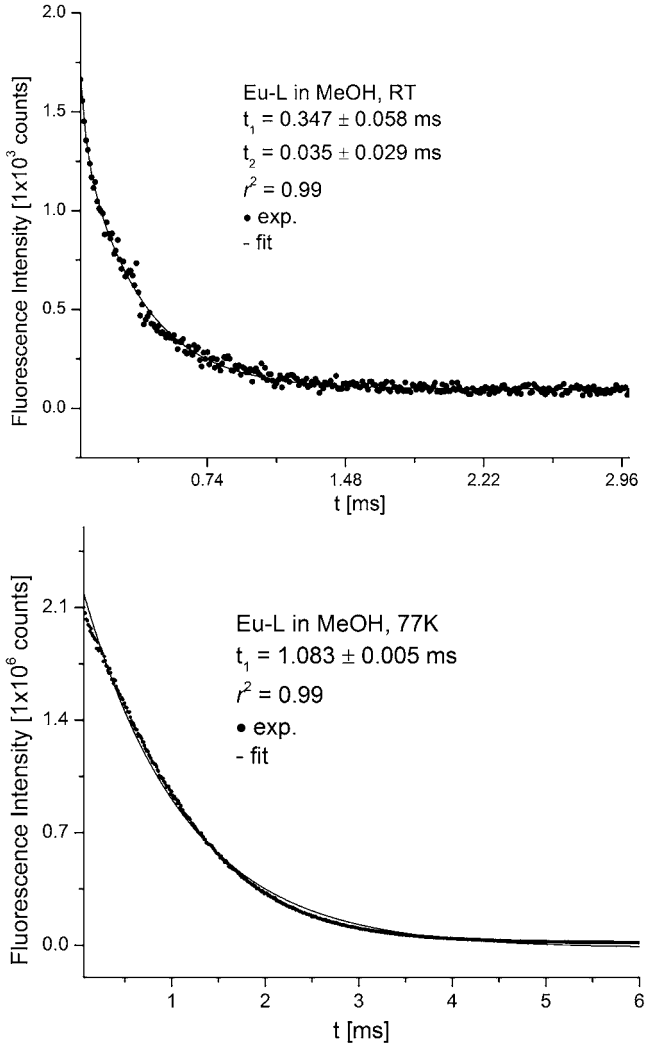

Figure 3. Representative luminescence lifetime decay curves for samples of **Eu-L** in MeOH at 298 K (top) and at 77 K (bottom).

of the emission lifetime at the expected europium(III) emission wavelength corresponding to the $^5D_0 \rightarrow {}^7F_4$ transition due to a small amount of ligand background emission still present near 700 nm; the decay in this case again becomes monoexponential upon cooling. In addition to limiting back-transfer, generation of the low-temperature matrix should limit the effect of nonradiative pathways resulting from molecular motion relative to the room temperature solution favoring enhanced metal-centered emission at 77 K. This type of nonradiative, vibrational quenching occurs, for example, through CH, NH, and most notably OH vibrations of ligands and solvent

Table 1. Photophysical Data of Complex Eu-L and the Complex Encapsulated within SiO_2 NPs, Eu-L@SiO_2[a]

	^1S [cm^{-1}][b]	^3T [cm^{-1}][b]	τ_{MeOH} [ms]	τ_{MeOD} [ms]	n[c]	τ_{MeOH} [ms][d]
Eu-L	20820 ± 410	17670 ± 170	0.347 ± 0.058	0.751 ± 0.019	3.3	1.063 ± 0.051
			0.035 ± 0.029	0.020 ± 0.001		
Eu-L@SiO_2	20620 ± 230	17730 ± 030	0.495 ± 0.091	1.000 ± 0.029	2.1	1.426 ± 0.048
			0.194 ± 0.103	0.215 ± 0.027		

[a]Lifetime measurements performed in methanol and deuterated methanol monitored at λ_{ex} = 315 nm and λ_{em} = 612 nm at 4.9 mg mL^{-1} for the complex and 2 mg mL^{-1} for the NPs with the encapsulated complex. [b]Singlet and triplet state measurements were performed in methanol with **Gd-L** and the NPs with encapsulated **Gd-L** at 77 K and are indicated as the 0–0 transitions. [c]Number of coordinated solvent molecules determined with Horrocks equation.[38] [d]Lifetime measured at 77 K.

dx.doi.org/10.1021/ic3022722 | Inorg. Chem. 2013, 52, 6311–6318

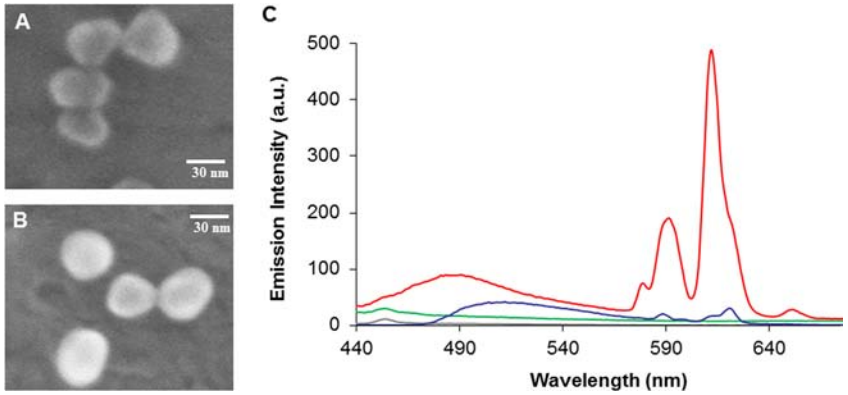

Figure 4. SEM and fluorescence characterization of the SiO_2 NPs: (A) SEM image of the empty SiO_2 NPs; (B) SEM image of the **Eu-L**@SiO_2 particles; (C) emission spectra at room temperature of the ethanol blank (gray), empty SiO_2 NPs at 10 nM (green), **Eu-L**@SiO_2 at 10 nM (red), and **Eu-L** free complex at 3 mM (blue) (EtOH solvent; λ_{ex} = 400 nm).

molecules present in the metal coordination sphere.[6,34] Measurement of the luminescence lifetime in the presence of a solvent such as methanol and comparison to the lifetime in deuterated methanol allow determination of the number of OH groups, and therefore methanol solvent molecules coordinated to the metal center, and give an indication of the magnitude of solvent-induced vibrational quenching.[38] Analogous to what is seen in methanol, in deuterated methanol the decay curve of the emission intensity can be fit to a double exponential, corresponding to metal-centered emission and ligand phosphorescence due to the back-energy-transfer process (see Table 1 for lifetime values). By using an equation proposed by Horrocks and co-workers,[38] it can be calculated that, on average, approximately three methanol molecules are present in the first coordination sphere of the metal ion. This is consistent with the structure of the complex shown in Scheme 1; in solution, molecules of a coordinating solvent such as methanol can easily replace the three bidentate nitrate anions.

Synthesis and Characterization of Eu-L@SiO_2 NPs. Noting the weak metal-centered luminescence intensity of **Eu-L** at room temperature, nanoencapsulation via silica formation was used to trap the complex within a NP matrix to restrict molecular motion through secondary interactions in an attempt to enhance metal emission without the need for decreased temperature. In addition to the potential effect on the photophysical properties, encapsulation within NPs would also limit leaching of the Ln ion in further potential bioassay or medical imaging applications. The SiO_2 NPs employed here were synthesized using a Stöber method, where TEOS was added to a sample containing the metal complex in a basic bulk ethanol solution.[39] Once formed, SEM images of the NPs were acquired (Figures 4A,B). Figure 4A shows the empty SiO_2 NPs (38.9 ± 5.8 nm), and Figure 4B displays the **Eu-L**-doped particles (40.7 ± 3.5 nm). Both images display particles that are quite uniform in size and tend to be spherical in shape. Importantly, the addition of **Eu-L** to the silica matrix does not appear to adversely affect particle formation. The number of europium centers per NP was determined to be 1273 ± 47 Eu/NP based on ICP-MS analysis of digested **Eu-L**@SiO_2.

As previously mentioned, leaching of the complex or Ln ion from the generated NPs would limit the applicability of such hybrid materials. Evaluation of the release of encapsulated **Eu-L** was therefore performed. Following the synthesis of **Eu-L**@SiO_2 particles, the samples were washed and suspended in fresh ethanol. The **Eu-L** complex is highly soluble in ethanol, while the silica matrix is not, making it an ideal choice for the experiment. After washing, the supernatant was collected from the mixture and an absorption spectrum collected, monitoring at 400 nm. This process was repeated on several samples over the course of 6 weeks with increasing exposure times of the NPs within the ethanol solvent. Figure S3 (Supporting Information) shows the absorbance data collected for a series of samples obtained over the 6-week period to evaluate the potential leaching of the metal complex into the supernatant. For all samples, the **Eu-L** absorption measurements were consistent with ethanol unexposed to the NPs, which represents the background level of the signal. This indicates that **Eu-L** leaching from the silica matrix of the NP was not observed over the 6-week period.

Because of a possible lack of sensitivity of UV−vis absorption analysis for the detection of free europium(III) ion in the leaching supernatant, ICP-MS analysis was also conducted with the samples. The detection of elements like europium with this technique is especially sensitive because of their high ionization efficiency, lack of isobaric interferences, and extremely low natural abundance. These factors combined lead to europium having a very low background signal, making the Ln readily detected in a sample. For the ICP-MS study, several samples were tested for the amount of europium present including a digested sample of the NPs to verify the presence of the metal inside the synthesized **Eu-L**@SiO_2 particles, the ethanol solution immediately after washing the prepared NPs, and the supernatant after incubation of the particles in ethanol for 6 weeks. The europium contents of freshly prepared samples of ethanol and Aqua Regia solutions were also examined as controls. A calibration curve of europium standards was also prepared for quantification of the europium levels present for each of the samples. The digestion conditions used on the NPs effectively dissolve the silica matrix of the particle, simulating a complete release of the europium contained within and allowing for quantification of the encapsulated Ln. This sample functions as a positive control, and a concentration of 346.9 ppb was measured via ICP-MS using a calibration curve generated from the series of europium standards. On the basis of this result, combined with the known limit of detection of 21.7 ppt for europium, ICP-MS would be able to detect europium leaching at levels of 0.0063% of the total europium present in the NPs. Analysis of the ethanol solution wash after exposure to the particles was below the detection limit of the instrument, indicating that europium is encapsulated inside the

dx.doi.org/10.1021/ic3022722 | Inorg. Chem. 2013, 52, 6311−6318

particle. After 6 weeks of incubation in ethanol, the amount of europium that leached from the NP was also below the detection limit of the instrument (Figure S3, Supporting Information). This indicates that the europium complex does not dissociate appreciably from the NP and the particles remain stable with regard to the europium content for a significant period of time.

Effect of Nanoencapsulation on Eu-L Luminescence. The effect of nanoencapsulation on the luminescence properties of **Eu-L** was determined by acquisition of the room temperature emission spectra shown in Figure 4. As the spectra reveal, encapsulating **Eu-L** within an SiO_2 NP enables significant metal emission at room temperature (Figure 4C, red) compared to the free complex (Figure 4C, blue). These spectra were obtained for solutions with concentrations of 10 nM for **Eu-L**@SiO_2 (2 mg mL^{-1} material) and 3 mM for the free complex (2 mg mL^{-1} **Eu-L**). A much higher concentration of the free complex relative to **Eu-L**@SiO_2 was required for the comparison because the free complex emission spectrum at 10 nM was not observable. The spectrum of the **Eu-L**@SiO_2 sample indicates strong metal emission with some less intense ligand emission still present. This spectrum resembles that of the free complex cooled to 77 K showing all expected europium(III) emission peaks, and the relatively intense peak at 615 nm is consistent with the observation of bright-red light emitted when the NP solution is exposed to UV light. Considering this europium emission peak, the emission intensity of the encapsulated complex (10 nM) compared to that of the free complex (3 mM) shows an enhancement factor of 6×10^6. While quantum yield measurements were not carried out here because it would not be possible to compare such results to the nonencapsulated complex, this enhancement factor based on the prominent metal emission peak reveals the significant effect of nanoencapsulation on the luminescence intensity.

Another effect of encapsulation becomes apparent in comparing the normalized emission intensities of free and encapsulated complexes as a function of the wavelength (Figure 5). Encapsulation leads to a significant broadening of the metal-centered emission bands, indicative of a less homogeneous coordination environment of the metal ion in its encapsulated

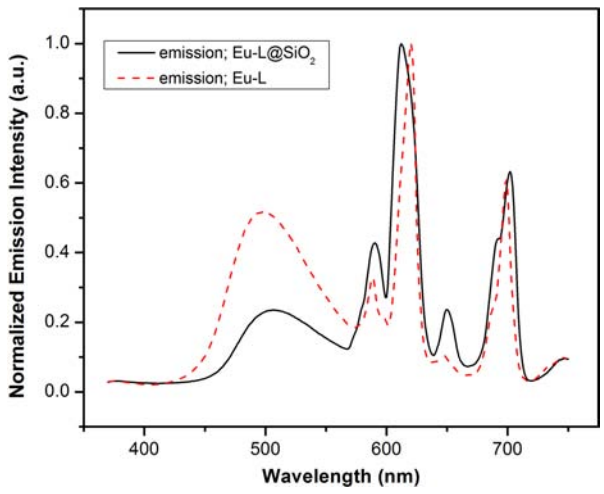

Figure 5. Normalized emission spectra of **Eu-L** in MeOH at 4.9 mg mL^{-1} of complex (red dashed line) and of **Eu-L**@SiO_2 in MeOH suspension (black solid line) at ~2 mg mL^{-1}.

form.[40] For example, the full width at half-maximum band assigned to the $^5D_0 \rightarrow {}^7F_2$ transition increases from 15 to 23 nm upon encapsulation of the complex. Analysis of this prominent peak is noted because of the potential to more easily discern the broadening relative to the other metal emission peaks observed. Probing this effect for the $^5D_0 \rightarrow {}^7F_0$ transition, in particular, is further complicated by the fact that this transition does not suffer broadening or splitting with the crystal field due to changes in symmetry because both states are nondegenerate, that is no multiplicity of the J value. Ligand phosphorescence of **Eu-L** is also shown to decrease upon encapsulation because of a decrease in vibration-mediated back-transfer. However, because of decreased vibrational contributions to all energy-transfer processes, the phosphorescence lifetime is considerably longer than that for the free complex. When the metal-centered emission lifetimes in methanol and deuterated methanol are compared (Table 1), approximately two methanol molecules are coordinated to the metal complex in the NPs, showing that, in addition to providing a rigid environment, the particles also prevent the diffusion of solvent molecules to the complex to a small extent. Finally, the singlet and triplet excited-state energies of the ligand (Table 1) are not modified in the encapsulation process, which further confirms that encapsulation of the complex in the SiO_2 NPs only affects the vibrationally mediated energy-transfer processes.

The increase in the rigidity of the ligand environment provided by encapsulation into the NPs is further seen through the shape and relative intensity of the singlet and triplet emission peaks of the ligand in the free and encapsulated forms. The two spectra, taken at 77 K, of the gadolinium analogue of **Eu-L** in solution and encapsulated gadolinium complex (**Gd-L**@SiO_2) are shown in Figure 6. In the case of the encapsulated

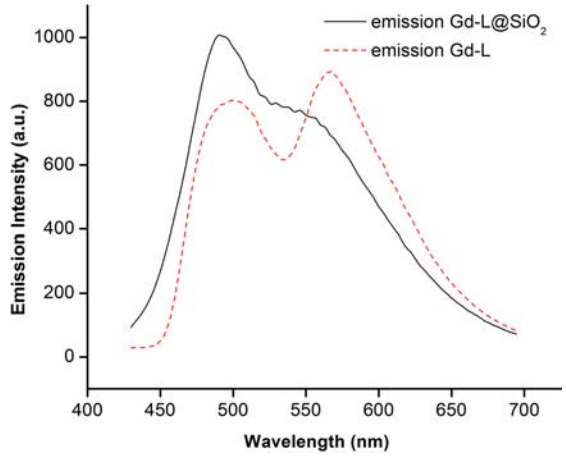

Figure 6. Emission spectra of **Gd-L** (red dashed line) and **Gd-L**@SiO_2 (black solid line) in MeOH at 77 K.

complex, the singlet emission is more pronounced than the triplet emission. Deconvoluting both spectra into their Franck–Condon progressions (Figure S4, Supporting Information) confirms that the singlet-to-triplet ratio is higher for the encapsulated **Gd-L** complex, consistent with less efficient nonradiative pathways contributing to the quenching of the singlet state. In the emissive **Eu-L**@SiO_2, this nonradiative quenching protection through encapsulation is, by analogy, also active. Despite the lower intersystem crossing efficiency observed due to diminished quenching of the singlet state, the metal-centered emission is still enhanced because of the

dx.doi.org/10.1021/ic3022722 | Inorg. Chem. 2013, 52, 6311–6318

decrease of vibrational quenching in the first coordination sphere of the metal ion as well as decreased back transfer, as discussed above.

CONCLUSION

In closing, we have reported a new europium complex employing the TIDP motif and the "turning on" of Ln-centered luminescence from the complex via nanoencapsulation within discrete particles. The complex can be readily synthesized in one convenient step in a metal-templated reaction and shows poor luminescence properties at room temperature. Embedding the complex within the SiO_2 NP matrix at room temperature induces the same low-temperature effect on europium-derived emission that is only seen for the free complex by cooling to 77 K. Noteworthy is the fact that the dramatic luminescence enhancement observed is achieved from relatively simple precursors assembled under ambient conditions. In addition, the NPs generated are robust with no signs of degradation or leaching of the complex with time. This combination of the straightforward synthesis, stability, and favorable photophysical properties under practical conditions, demonstrated here for Ln-TIDP complexes for the first time, reveals the promise of such materials in future applications such as bioassay work. Ongoing efforts in our laboratory include the development of new TIDP derivatives to further promote metal-centered emission and potential utility of this unique type of nanomaterial.

ASSOCIATED CONTENT

Supporting Information

IR and UV−vis absorption spectra of **Eu-L**, plots of complex leaching study results, and deconvolution of the 77 K emission spectra for free and nanoencapsulated **Gd-L**. This material is available free of charge via the Internet at http://pubs.acs.org.

AUTHOR INFORMATION

Corresponding Author

*E-mail: josh.smith.ctr@wpafb.af.mil (J.E.S.), ewerner@ut.edu (E.J.W.).

Author Contributions

The manuscript was written through contributions of all authors. All authors have given approval to the final version of the manuscript.

Notes

The authors declare no competing financial interest.

ACKNOWLEDGMENTS

Financial support for this work from the College of Science and Technology (SRS Program, AASU), the Department of Chemistry and Physics (AASU), the Department of Chemistry, Biochemistry and Physics (UT), the University of Nevada, Reno, and Grant NSF-CHE1058805 (to A.d.B.-D.) is acknowledged. The SEM work was performed at the Georgia Tech Nanotechnology Research Center, a member of the NSF supported National Nanotechnology Infrastructure Network, and the authors thank Dr. David Gottfried for assistance in obtaining the images.

REFERENCES

(1) Ananias, D.; Kostova, M.; Almeida Paz, F. A.; Ferreira, A.; Carlos, L. D.; Klinowski, J.; Rocha, J. *J. Am. Chem. Soc.* **2004**, *126*, 10410−10417.
(2) Carlos, L. D.; Ferreira, R. A. S.; de Zea Bermudez, V.; Ribeiro, S. J. L. *Adv. Mater.* **2009**, *21*, 509−534.
(3) Carlos, L. D.; Ferreira, R. A. S.; de Zea Bermudez, V.; Julián-López, B.; Escribano, P. *Chem. Soc. Rev.* **2011**, *40*, 536−549.
(4) Escribano, P.; Julián-López, B.; Planelles-Aragó, J.; Cordoncillo, E.; Viana, B.; Sanchez, C. *J. Mater. Chem.* **2008**, *18*, 23−40.
(5) Wang, F.; Chatterjee, D. V.; Li, Z.; Zhang, Y.; Fan, X.; Wang, M. *Nanotechnology* **2006**, *17*, 5786−5791.
(6) Bünzli, J.-C. G.; Piguet, C. *Chem. Soc. Rev.* **2005**, *34*, 1048−1077.
(7) Samuel, J.; Tallec, G.; Cherns, P.; Ling, W. L.; Raccurt, O.; Poncelet, O.; Imbert, D.; Mazzanti, M. *Chem. Commun.* **2010**, *46*, 2647−2649.
(8) Li, S.; Song, H.; Li, W.; Lu, S.; Ren, X. *J. Nanosci. Nanotechnol.* **2008**, *8*, 1272−1278.
(9) Jiang, S.; Zhang, Y.; Lim, K. M.; Sim, E. K. W.; Ye, L. *Nanotechnology* **2009**, *20*, 155101−155109.
(10) Moran, C. E.; Hale, G. D.; Halas, N. J. *Langmuir* **2001**, *17*, 8376−8379.
(11) Petit, L.; Griffin, J.; Carlie, N.; Jubera, V.; García, M.; Hernández, F. E.; Richardson, K. *Mater. Lett.* **2007**, *61*, 2879−2882.
(12) Yu, M.; Lin, J.; Fang, J. *Chem. Mater.* **2005**, *17*, 1783−1791.
(13) Choi, J.; Kim, J. C.; Lee, Y. B.; Kim, I. S.; Park, Y. K.; Hur, N. H. *Chem. Commun.* **2007**, 1644−1646.
(14) Massue, J.; Quinn, S. J.; Gunnlaugsson, T. *J. Am. Chem. Soc.* **2008**, *130*, 6900−6901.
(15) Soares-Santos, P. C. R.; Nogueira, H. I. S.; Félix, V.; Drew, M. G. B.; Sá Ferreira, R. A.; Carlos, L. D.; Trindade, T. *Chem. Mater.* **2003**, *15*, 100−108.
(16) Chen, Y.; Lu, Z. *Anal. Chim. Acta* **2007**, *587*, 180−186.
(17) Driesen, K.; Deun, R. V.; Görller-Walrand, C.; Binnemans, K. *Chem. Mater.* **2004**, *16*, 1531−1535.
(18) Li, H.; Inoue, S.; Machida, K.; Adachi, G. *Chem. Mater.* **1999**, *11*, 3171−3176.
(19) Morita, M.; Rau, D.; Kai, T. *J. Lumin.* **2002**, *100*, 97−106.
(20) Guodong, Q.; Minquan, W. *J. Phys. Chem. Solids* **1997**, *58*, 375−378.
(21) Gao, J.; Reibenspies, J. H.; Martell, A. E. *Angew. Chem., Int. Ed.* **2003**, *42*, 6008−6012.
(22) Roznyatovsky, V. V.; Borisova, N. E.; Reshetova, M. D.; Ustynyuk, Y. A.; Aleksandrov, G. G.; Eremenko, I. L.; Moiseevb, I. I. *Russ. Chem. Bull., Int. Ed.* **2004**, *53*, 1208−1217.
(23) Bag, P.; Dutta, S.; Flörke, U.; Nag, K. *J. Mol. Struct.* **2008**, *891*, 408−419.
(24) Gagné, R. R.; Spiro, C. L.; Smith, T. J.; Hamann, C. A.; Thies, W. R.; Shiemke, A. K. *J. Am. Chem. Soc.* **1981**, *103*, 4073−4081.
(25) Huang, W.; Gou, S.; Hu, D.; Meng, Q. *Synth. Commun.* **2000**, *30*, 1555−1561.
(26) Crosby, G. A.; Whan, R. E.; Alire, R. M. *J. Chem. Phys.* **1961**, *34*, 743−748.
(27) Kumar, D. S.; Alexander, V. *Polyhedron* **1999**, *18*, 1561−1568.
(28) d'Hardemare, A. M.; Philouze, C.; Jarjayes, O. *Acta Crystallogr.* **2006**, *E62*, m227−m228.
(29) Bag, P.; Flörke, U.; Nag, K. *Dalton Trans.* **2006**, 3236−3248.
(30) Kumar, D. S.; Alexander, V. *Inorg. Chim. Acta* **1995**, *238*, 63−71.
(31) Carnall, W. T.; Siegel, S.; Ferraro, J. R.; Tani, B.; Gebert, E. *Inorg. Chem.* **1973**, *12*, 560−564.
(32) Aruna, V. A. J.; Alexander, V. *J. Chem. Soc., Dalton Trans.* **1996**, 1867−1873.
(33) Muller, G.; Maupin, C. L.; Riehl, J. P.; Birkedal, H.; Piguet, C.; Bünzli, J.-C. G. *Eur. J. Inorg. Chem.* **2003**, 4065−4072.
(34) de Bettencourt-Dias, A. *Curr. Org. Chem.* **2007**, *11*, 1460−1480.
(35) Berezin, M. Y.; Achilefu, S. *Chem. Rev.* **2010**, *110*, 2641−2684.
(36) Kocher, J.; Gumy, F.; Chauvin, A.-S.; Bünzli, J.-C. G. *J. Mater. Chem.* **2007**, *17*, 654−657.
(37) Sambrook, M. R.; Curiel, D.; Hayes, E. J.; Beer, P. D.; Pope, S. J. A.; Faulkner, S. *New J. Chem.* **2006**, *30*, 1133−1136.
(38) Holz, R. C.; Chang, C. A.; Horrocks, W. D. *Inorg. Chem.* **1991**, *30*, 3270−3275.

(39) Smith, J. E.; Medley, C. D.; Tang, Z.; Shangguan, D.; Lofton, C.; Tan, W. *Anal. Chem.* **2007**, *79*, 3075−3082.
(40) Iwu, K. O.; Soares-Santos, P. C. R.; Nogueira, H. I. S.; Carlos, L. D.; Trindade, T. *J. Phys. Chem. C* **2009**, *113*, 7567−7573.